Nitrogen in graphite and carbon nanotubes: Magnetism and mobility

Yuchen Ma,* A. S. Foster, A. V. Krasheninnikov, and R. M. Nieminen
Laboratory of Physics, Helsinki University of Technology, P.O. Box 1100, Helsinki 02015, Finland
(Received 15 June 2005; revised manuscript received 6 September 2005; published 11 November 2005)

We use *ab initio* methods to study the atomic, electronic, and magnetic structure of nitrogen impurities in graphite and carbon nanotubes. We show that the probable configurations for the N impurity atoms are bridgelike adatoms on graphene sheets/nanotubes, substitutional sites and intercalated N_2 molecules. We further calculate the migration energy barrier for an N adatom on the graphite surface and the activation energy for the coalescence of two N adatoms into a molecule, which are 1.1 eV and 0.8 eV, respectively. We also find that the N adatom has a magnetic moment of $0.6\mu_B$ and that substitutional N enhances the magnetism of C adatoms on graphite and nanotubes, acting as a general promoter of magnetism in carbon systems.

DOI: 10.1103/PhysRevB.72.205416 PACS number(s): 75.50.Dd, 85.40.Ry, 81.05.Uw

I. INTRODUCTION

Incorporation of nitrogen into sp^2-hybridized carbon materials has been shown to be a promising way to change the mechanical and electronic properties of the material in a controllable manner. In particular, N-doped fullerenes have been found to exhibit a high hardness combined with a high elasticity due to cross-linking between curved basal planes.[1] Likewise, N doping of carbon nanotubes (CNTs)[2] can give rise to nanotube functionalization[3] and other changes in the structure, e.g., transformations of the atomic network to bamboolike structures,[4,5] which can enhance field emission[6] from the nanotubes.

An additional motivation for studies on nitrogen doping of CNTs is the idea that nitrogen substitutional impurities can provide more control over the nanotube electronic structure,[3–13] as the N atom has roughly the same atomic radius as C, while it possesses one electron more than C. One can expect that nitrogen atoms should provide extra electrons and thus make all the tubes metallic, even if the original tubes were narrow-band semiconductors. This is of particular importance because as-grown CNTs represent a mixture of metallic and semiconducting tubes, and specific chiral control remains lacking.

Nitrogen impurities in π-conjugated systems can, in principle, affect the magnetic properties of the material as well.[14] This is a very interesting point, as the origin of the magnetic signal experimentally observed in various carbon systems[15–19] is still unclear. In addition to the existing theories which explain magnetism in terms of undercoordinated atoms (defects)[20–25] and special topology of the carbon atomic network,[26] one cannot exclude a contribution from impurities of light chemical elements which are nonmagnetic by themselves. Indeed, as experiments[27,28] and theoretical calculations[29–32] show, hydrogen atoms may play an important role in the magnetism of graphite, fullerenes and CNTs. Nitrogen may be important as well, whether intentionally or unintentionally introduced, as it can give rise to local spins and facilitate the development of the long-range magnetic order.

Irrespective of the magnetic properties of carbon systems, knowing the details of the interaction of N impurities with CNTs is also very important for understanding and optimizing the nanotube doping process. Several methods based on arc-discharge techniques[4,33] or substitutional reactions[10] are used nowadays to produce nitrogen-doped CNTs. Similar to the doping of graphite[34] and fullerene solids,[35] irradiation[36] can be used to introduce N impurities. Independent of the method used, the key issue is the mobility of N atoms and formation of molecules intercalated between graphite layers.[12]

Following these two motivational directions, we report first principles studies of the magnetic properties of N impurities in graphite and CNTs, and of their migration and coalescence into molecules.

II. METHOD

The calculations have been performed using the periodic plane wave basis VASP (Refs. 37 and 38) code, implementing the spin-polarized density functional theory (DFT) and the generalized gradient approximation of Perdew and Wang.[39] We have used projected augmented wave (PAW) potentials[40,41] to describe the core ($1s^2$) electrons. A kinetic energy cutoff of 400 eV was found to converge the total energy of our systems to within meV.

For a N atom on a single graphene layer, a 50-atom slab was used. For studying N on CNTs, (5, 5), (7, 0), and (9, 0) single-walled carbon nanotubes (SWNTs) were chosen, the unit cells contained 60, 56, and 72 atoms, respectively. Periodical boundary conditions were applied along the graphene surface and the axial direction of SWNTs. Supercells were constructed with adequate vacuum gaps between adjacent graphene layers and adjacent tubes in the radial direction so that interaction between images was negligible. We used five Monkhorst-Pack k-points[42] (Γ-point included) for the Brillouin zone integration for graphene and four for nanotubes. The minina of the total energy were found using a conjugate gradient algorithm. All atoms are fully relaxed until the change in energy upon ionic displacement is below 1 meV.

The adsorption energy E_{ads} of an adatom (N or C) on a substrate (graphene or nanotube) is calculated from $E_{\mathrm{ads}} = E_{\mathrm{sub\text{-}adatom}} - (E_{\mathrm{sub}} + E_{\mathrm{adatom}})$, where E_{sub}, E_{adatom}, and $E_{\mathrm{sub\text{-}adatom}}$ are the energies of the substrate, the adatom, and the substrate-adatom system, respectively. The atomic

ground states of N and C atoms are a quartet and a triplet state, respectively. We used the energies of these states as references to calculate the adsorption energies.

III. RESULTS AND DISCUSSION

A. Substitutional and adatom nitrogen impurities

We first studied the magnetic properties of the perfect sp^2 substitutional N impurity in the graphitic network, as this is the most stable configuration. The substitutional N atom is sp^2-hybridized, as for lattice carbons, and the remaining two electrons participate in the π-electron network of C atoms. For nanotubes the behavior of the dopant electron depends on the chirality, with complete delocalization on metallic tubes [(9,0) and (5,5)] and limited localization on the semiconducting tube. In contrast to previous studies,[3] despite relative agreement in the localization of the defect state, we found that the ground state of substitutional nitrogen was always nonmagnetic even when beginning with a magnetic guess configuration. In order to check that this was not a result of the density of the defects, we considered (7,0) nanotubes up to 43 Å in length and observed no change in the result. We also further considered an (8,0) nanotube of 43 Å in length, but did not observe the localization of a finite spin density within 30 Å reported in Ref. 3. The only clear difference between the two approaches is the use of ultrasoft pseudopotentials in Ref. 3 as opposed to the PAW potentials used in our work. Since we do not have information on the specific pseudopotentials they used, we can only assume that the more general PAW approach is accurate.

If a N dopant does not occupy the substitutional sp^2 site in the graphitic network, it will be absorbed on the surface of a CNT and/or graphite microcrystal or intercalated between graphene layers. Indeed, as experiments demonstrate, instead of occupying the substitutional sp^2 position in the graphitic network, a substantial part of the dopant is chemisorbed[43] on the nanotube surface, forms nitrogen molecules intercalated between graphite layers,[12] or binds to irregular carbon structures in sp^3 sites.[4] The intercalated N atom can crosslink between graphene layers[11] or form bonds with a single graphene layer, depending on the distance between the layers (in the bundles of single-walled nanotubes) and the local stacking type.

The properties of N impurities intercalated between graphite layers are determined by not only local covalent bonding but also long-range changes in the interlayer separation, i.e., by van der Waals-type interactions. Since van der Waals interactions are poorly described within DFT with LDA or GGA,[44,45] here we only consider the case when the N dopant forms bonds with a single graphene layer. However, we think that the overall behavior of N impurities between graphitic layers is correctly reproduced by this model, as the covalent interaction is much stronger than the weak van der Waals forces.

The N adatom forms a bridgelike structure on the graphene surface, as shown in Fig. 1(a). This is similar to the behavior of the carbon and oxygen adatoms on the graphene surface.[46,47] The length of the C-N bond is 1.45 Å and the length of the bond between the two C atoms bonded to the N is 1.58 Å. These two C atoms become sp^3-hybridized. The adsorption energy is 0.93 eV, and this structure has a magnetic moment of $0.57\mu_B$. Figure 1(b) shows the distribution of spin-polarization, most of which comes from the p orbital of the N adatom, which is perpendicular to the C-N-C plane.

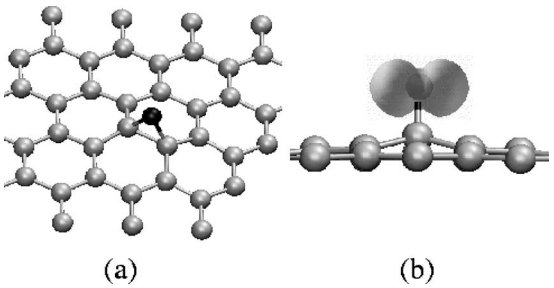

FIG. 1. (a) Equilibrium position of a N adatom on the graphene surface. (b) The isosurface of the spin density at the value of 0.05 $e/\text{Å}^3$. The grey spheres and black sphere represent C and N atoms, respectively.

On the outer surface of CNTs, N adatoms also form bridgelike structures with two C atoms.[43] Due to the inequivalence of adjacent C-C bonds on the wall of nanotubes,

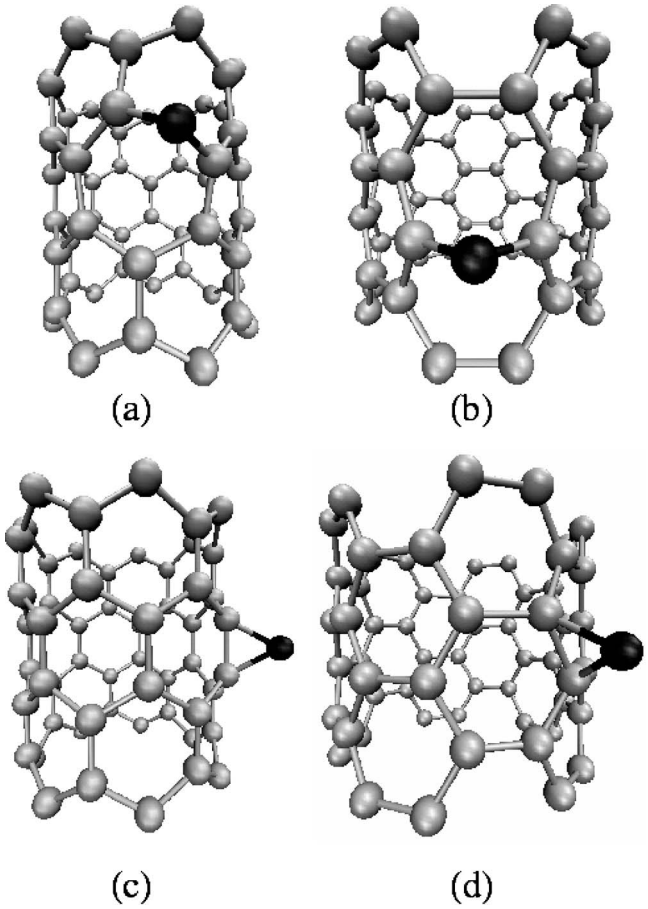

FIG. 2. Equilibrium positions of the N adatom on SWNTs. (a) "Perpendicular" position on zigzag SWNTs; (b) "perpendicular" position on armchair SWNTs; (c) "parallel" position on zigzag SWNTs; (d) "parallel" position on armchair SWNTs; the grey and black spheres represent C and N atoms, respectively.

there are two kinds of bridgelike structures on both the zigzag [(7, 0) and (9, 0)] and armchair [(5, 5)] tubes as shown in Fig. 2. These two kinds of structures are termed "perpendicular" and "parallel," respectively, according to the orientation of the bridge plane relative to the axis of the tube. For the (7, 0), (9, 0), and (5, 5) tubes, the "perpendicular" configuration is lower in energy than the "parallel" one. In the "perpendicular" configuration, the N adatom pushes the two bonding C atoms apart, and the bond between these two C atoms is broken. Table I gives the magnetic moment and adsorption energy of each configuration for each tube. Every configuration has a finite magnetic moment. Similar to the N adatom on graphene, the magnetic moment of the tube mainly comes from the p orbital of the N adatom. In general, the magnitude of the magnetic moment is related to the coupling of this p orbital with the surface π orbitals—the larger the coupling the smaller the moment.

Comparing the magnetic moments of these three tubes, we find that the magnetic moments of the "perpendicular" configuration are smaller than those of the "parallel" one for all three tubes. This is due to the difference in structure induced by the impurity, i.e., the C-C bond is broken for the perpendicular configuration resulting in a much stronger coupling between the orbitals of the N adatom and the carbon system, reducing the moment.

The magnetic moment of every configuration of the (7, 0) tube is larger than that of the same configuration for (9, 0) and (5, 5) tubes. From zone-folding arguments, perfect (7, 0), (9, 0) and (5, 5) SWNTs are semiconducting, metallic and metallic, respectively (noting that graphite is a semimetal). The more delocalized orbitals in the metallic systems couple more strongly to the N adatom's p orbital reducing the moment. This behavior contrasts with that seen for a C adatom,[46,48] as carbon has two unpaired orbitals involved in the magnetic moment, whereas nitrogen's lone pair saturates two, leaving only a single unpaired orbital.

B. N adatom diffusion and N_2 formation

Having calculated the minimum energy configuration for a N adatom on graphene surface, we evaluated the energy barrier for the adatom to migrate to a adjacent equilibrium bridgelike position. The calculations were done by the nudged elastic band method[49] implemented into VASP to determine minimum-barrier diffusion paths between known initial and final geometries. The nudged elastic band method starts from a chain of geometries interpolating between the initial and the final geometries. Then the atomic configurations in the different geometries are iteratively optimized using only the ionic-force components perpendicular to the hypertangent.

The migration barrier is 1.1 eV with the migration path being nearly a straight line connecting the original and final equilibrium positions of the adatom. This relatively low migration energy means the N adatom should be highly mobile at high temperatures (over 900 K) used for C-N nanotube growth (in our estimate we assume that the jump frequency of the N adatom is close to the jump frequency of a C interstitial in graphite[50]), but of limited mobility at room temperature. However, for N interstitials intercalated in graphite the presence of a nearby layer may lower the migration barrier.

N adatoms on graphene surface may coalesce to form N_2 molecules. Figure 3 shows the coalescence process of two N adatoms. The simulation is done by constrained molecular dynamics. The projected distance between the two N atoms on the graphene plane is fixed at each step. The simulation starts from the structure (I) which is the local stable state just before the reaction. Both N atoms form bridgelike structures at this step. Structure (II) is the maximum energy state during the reaction, where one N atom forms a bridgelike structure while the other has only a single bond with graphene. Structures (III) and (IV) are the states when the projected distance between the N atoms are 1.9 Å and 1.5 Å, respectively. At 1.9 Å [stage (III)], each both N atoms have only a single bond with the graphene surface. At 1.5 Å, a N_2 molecule has been formed and it leaves the graphene surface (the bond length of a free N_2 molecule is 1.11 Å). The activation energy for this reaction is 0.80 eV.

On the wall of CNTs, the migration of N adatoms and the N+N coalescence are more complicated and are related to the diameter of the tube. The general tendency is that the

TABLE I. Magnetic moment and adsorption energy of N adatoms (N-ad), C adatoms (C-ad) and C adatom-substitutional N atom pairs (as shown in Fig. 4) on the surface of graphene and SWNTs.

		Magnetic moment (μ_B)			Adsorption energy (eV)	
		N-ad	N-sub+C-ad	C-ad	N-ad	N-sub+C-ad
Graphite		0.57	0.98	0.45[a]	0.93	2.39
(7, 0)	Perp.	0.70	0.93	0.01	2.45	3.51
	Par.	0.97			2.05	
(9, 0)	Perp.	0.51	1.00	0.35[b]	2.21	3.42
	Par.	0.73			1.83	
(5, 5)	Perp.	0.59	0.92	0.44[b]	2.82	4.14
	Par.	0.71			1.67	

[a]Reference 46.
[b]Reference 48.

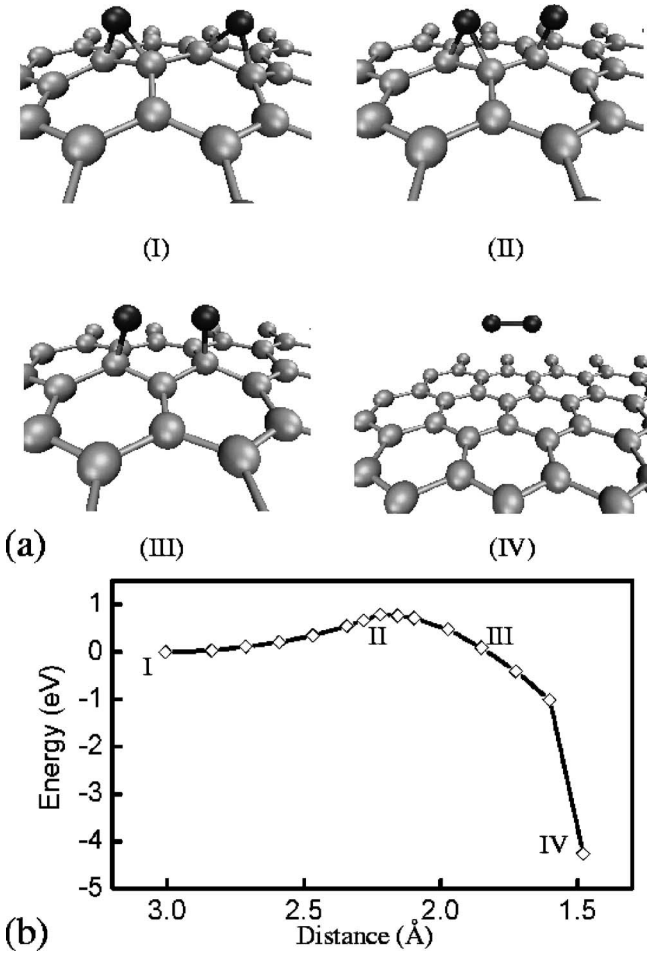

FIG. 3. (a) Coalescence process of two single N adatoms into a N_2 molecule and the corresponding potential-energy profile as a function of the projected distance between the N atoms on the graphene plane. (I) Local stable configuration before the coalescence start. (II) Maximum energy state during the coalescence process. (III) Intermediate configuration with the distance between the N atoms being 1.9 Å. (IV) N_2 molecule is formed and leaves the graphene surface. (b) Energy of the coalescence process given with respect to configuration (I).

migration barrier of adatoms on the outer nanotube surface increases with the decrease in the diameter of the nanotube.[51] On locally highly distorted sites of graphene or on small-diameter nanotubes, such as those in Figs. 2(a) and 2(b), the mobility of N adatom is low and the N adatom might be pinned at these sites. N atoms intercalated between graphene layers have been observed in graphite after nitrogen irradiation[52] and in carbon nanotubes after nitrogen plasma treatment.[11]

C. Substitutional nitrogen-carbon adatom pairs

During the production process of CNx films or nanotubes by substitutional reaction methods, after N plasma treatment, and especially after irradiation of the originally pristine carbon material with N ions, a number of C atoms can take interstitial positions. The interaction of C interstitials with substitutional N impurities has never been studied before.

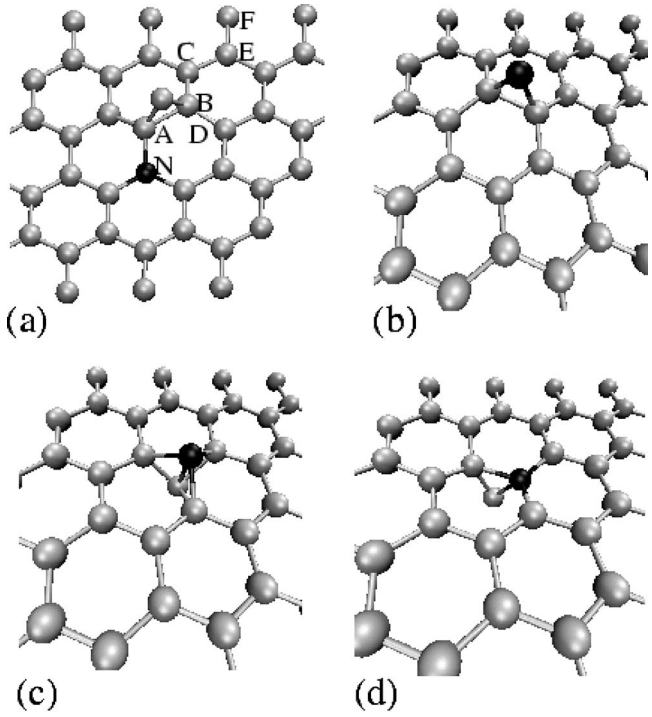

FIG. 4. (a) Graphene sheet with a substitutional N atom and a C adatom. Migration path (b)⇒(c)⇒(d) from a graphene layer with a N adatom (b) to a graphene with a substitutional N atom and a C adatom (d). The N atom "pushes" down one of the underlying C atoms and forms a "dumbell" at the saddle point (c). The grey and black spheres represent C and N atoms, respectively.

The ground state of a C adatom on the graphene surface is a bridgelike structure.[46] To find the minimum energy configuration of the C-adatom-N-impurity pair, we placed a C adatom at six different bridge positions above the bonds N-A, A-B, B-C, B-D, C-E, and E-F, as shown in Fig. 4(a). To fully understand the transformations which may happen to N impurities and intrinsic defects in graphite and nanotubes, we also considered the possible exchange of a N adatom with one of the C atoms bonded to the adatom. Figure 4 shows the start configuration (b) with the lowest energy and the final configuration (d), which is metastable, along with the transition point along the path (c).

The full energy landscape of the C adatom migration is shown in Fig. 5(a). Clearly the most stable configuration is for the carbon lattice to be restored by forming a N adatom—the barrier for exchange with N from this configuration is almost 4 eV. The most stable site for an existing C adatom near substitutional N is actually at site A-B (the structure " N-sub+C-ad" denoted in Table I). The adsorption energy at A-B (2.39 eV—see Table I) is larger than the adsorption energy of a C adatom on the pure graphene surface by 0.83 eV.[46] The barrier between A-B and N-A is about 0.7 eV, but the opposite migration has a barrier of less than 0.1 eV—hence the real barrier for a C adatom to exchange with a substitutional N is about 1.4 eV. This is inaccessible at room temperature, so the C adatom-substitutional N defect complex is stable.

The barrier for C to migrate to the next site away from substitutional N is about 0.8 eV, and this barrier tends to the

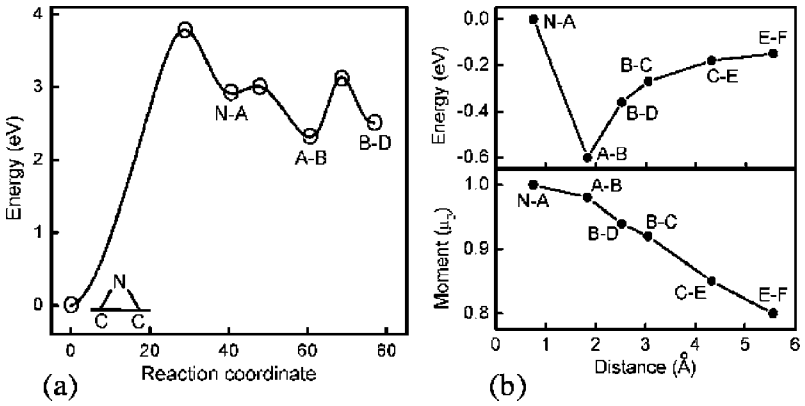

FIG. 5. (a) Energy landscape for migration of a C adatom near to a substitutional N site. The labels correspond to those configurations shown in Fig. 4(a), apart from reaction coordinate zero, where the C adatom replaces the substitutional N, resulting in a N adatom. Energy is given with respect to the lowest energy state. (b) Adsorption energy and magnetic moment of the C adatom at different sites on the graphene sheet. Energy is given with respect to configuration N-A. The x coordinate is the projected distance between the N atom and the C adatom on the graphene plane.

value for ideal graphene [0.45 eV (Ref. 46)] as the adatom travels further from N. Also, the general trend is that it is easier to approach the substitutional N site than retreat from it until the C adatom reaches the stable A-B position.

For all the configurations, the magnetic moments are nearly twice as large as that of a C adatom on a pure graphite sheet ($0.45\mu_B$).[46] The moment slightly depends on the distance of the C adatom from N, with a decrease of about $0.2\mu_B$ at the site E-F position [see Fig. 5(b)]. The substitutional N atom also enhances the magnetization of the C adatom on nanotubes (see Table I). In all cases the distribution of the magnetization is similar to that shown in Fig. 1(b).

The reason for the magnetization enhancement is as follows: Two of the four valence electrons of the C adatom participate in the covalent bonds with the C/N atoms in the substrate. One electron goes to the dangling sp^2 bond. The other is shared between the dangling sp^2 bond and the p orbital perpendicular to the bridge plane.[46] The dangling sp^2 orbital is much more prone to form bands with the surface π orbitals than the perpendicular p orbital. The more electrons can be supplied by the substrate to form bands with the dangling sp^2 orbital, the less electrons will be needed from the p orbitals, and thus more electrons of the p orbital will be spin-polarized. Comparing with the surfaces of pristine graphite and carbon nanotubes, a substitutional N atom near the C adatom can supply more electrons to form bands with the dangling sp^2 orbitals. This explains the enhancement of the spin-polarization of the C adatom by substitutional N.

IV. CONCLUSIONS AND OUTLOOK

Density-functional theory has been used to study the migration of a N adatom on the graphene surface and to investigate the contribution of N impurities to the magnetism observed in graphitic systems. Substitutional N atoms in both graphite and carbon nanotubes do not support any magnetic moment. However, N adatoms on the surfaces of graphite and CNTs have localized magnetic moments. We further studied the stability of various impurity configurations and showed that although single-atom N impurities are metastable with respect to the coalescence into N_2 molecules, followed by possible desorption from the sample, many magnetic impurity and/or intrinsic carbon defect configurations may survive at room temperature. Thus, if graphite or CNTs are irradiated with N ions, it is likely that a host of metastable substitutional N sites, vacancies and C adatoms will be created.[36]

Our results also show that substitutional N impurities act as stable attractors for mobile C adatoms, forming magnetic defect complexes. If we assume that the concentration of N impurities is 1 ppm and that all the local magnetic moments contribute to the macroscopic magnetic state, the graphitic sample should have the macroscopic magnetic moment M of around 10^{-3} emu/g. Correspondingly, an impurity concentration of 1000 ppm should provide $M \sim 1$ emu/g. Such an impurity concentration can easily be achieved by N implantation onto a thin (submicrometer) graphitic and/or nanotube sample. For example, an irradiation dose of 10^{16} N ions/cm^{-2} with energies 10–700 keV (to guarantee relatively smooth distribution of the implant atoms in the sample) would give an impurity concentration of 1000 ppm in a micrometer-thick sample. These values are in good agreement with recent nitrogen irradiation experiments on nanodiamond samples.[53] In that experimental work high-energy (100 keV) nitrogen ions were implanted in nanosized diamond (which is graphitized at high irradiation dose). Magnetic measurements on the doped samples showed ferromagnetic order at room temperature.

Given that much work has been done to study the magnetic properties of transition metals adsorbed on graphite and SWNTs to pursue low-dimensional nanomagnets,[54–57] our results also imply that thin (~100 nm) CN films or nanotubes may be a very attractive alternative to pure carbon systems.

ACKNOWLEDGMENTS

This research has been supported by the Academy of Finland Centre of Excellence Program (2000–2005) and partially by the ELENA project within the Academy of Finland TULE programme. The authors are grateful to the Centre of Scientific Computing, Espoo for computational resources.

*Electronic address: yma@fyslab.hut.fi; www.fyslab.hut.fi

[1] S. Stafström, Appl. Phys. Lett. **77**, 3941 (2000).
[2] *Carbon Nanotubes, Synthesis, Structure, Properties and Applications*, edited by M. S. Dresselhaus, G. Dresselhaus, and P. Avouris (Springer, Berlin, 2001).
[3] A. H. Nevidomskyy, G. Csányi, and M. C. Payne, Phys. Rev. Lett. **91**, 105502 (2003).
[4] R. Droppa, Jr., C. T. M. Ribeiro, A. R. Zanatta, M. C. dos Santos, and F. Alvarez, Phys. Rev. B **69**, 045405 (2004).
[5] J. W. Jang, C. E. Lee, S. C. Lyu, T. J. Lee, and C. J. Lee, Appl. Phys. Lett. **84**, 2877 (2004).
[6] R. C. Che, L.-M. Peng, and M. S. Wang, Appl. Phys. Lett. **85**, 4753 (2004).
[7] Y. Miyamoto, M. L. Cohen, and S. G. Louie, Solid State Commun. **102**, 605 (1997).
[8] R. Czerw *et al.*, Nano Lett. **1**, 457 (2001).
[9] M. Terrones *et al.*, Appl. Phys. A: Mater. Sci. Process. **65**, 355 (2002).
[10] D. Srivastava, M. Menon, C. Daraio, S. Jin, B. Sadanadan, and A. M. Rao, Phys. Rev. B **69**, 153414 (2004).
[11] L. H. Chan, K. H. Hong, D. Q. Xiao, T. C. Lin, S. H. Lai, W. J. Hsieh, and H. C. Shih, Phys. Rev. B **70**, 125408 (2004).
[12] H. C. Choi, S. Y. Bae, J. Park, K. Seo, C. Kim, B. Kim, H. J. Song, and H.-J. Shin, Appl. Phys. Lett. **85**, 5742 (2004).
[13] H. S. Kang and S. Jeong, Phys. Rev. B **70**, 233411 (2004).
[14] I. Hagiri, N. Takahashi, and K. Takeda, J. Phys. Chem. A **108**, 2290 (1994).
[15] T. L. Makarova, B. Sundqvist, R. Höhne, P. Esquinazi, Y. Kopelevich, P. Scharff, V. A. Davydov, L. S. Kashevarova, and A. V. Rakhmanina, Nature (London) **413**, 716 (2001).
[16] P. Esquinazi, A. Setzer, R. Höhne, C. Semmelhack, Y. Kopelevich, D. Spemann, T. Butz, B. Kohlstrunk, and M. Lösche, Phys. Rev. B **66**, 024429 (2002).
[17] J. M. D. Coey, M. Venkatesan, C. B. Fitzgerald, A. P. Douvalis, and I. S. Sanders, Nature (London) **420**, 156 (2002).
[18] A. V. Rode, E. G. Gamaly, A. G. Christy, J. G. Fitz Gerald, S. T. Hyde, R. G. Elliman, B. Luther-Davies, A. I. Veinger, J. Androulakis, and J. Giapintzakis, Phys. Rev. B **70**, 054407 (2004).
[19] B. Narymbetov, A. Omerzu, V. Kabanov, M. Tokumoto, H. Kobayashi, and D. Mihailovic, Nature (London) **407**, 883 (2000).
[20] Y. H. Kim, J. Choi, K. J. Chang, and D. Tománek, Phys. Rev. B **68**, 125420 (2003).
[21] A. N. Andriotis, M. Menon, R. M. Sheetz, and L. Chernozatonskii, Phys. Rev. Lett. **90**, 026801 (2003).
[22] M. Fujita, K. Wakabayashi, K. Nakada, and K. Kusakabe, J. Phys. Soc. Jpn. **65**, 1920 (1996).
[23] Y. Shibayama, H. Sato, T. Enoki, and M. Endo, Phys. Rev. Lett. **84**, 1744 (2000).
[24] K. Nakada, M. Fujita, G. Dresselhaus, and M. S. Dresselhaus, Phys. Rev. B **54**, 17954 (1996).
[25] K. Kusakabe and M. Maruyama, Phys. Rev. B **67**, 092406 (2003).
[26] N. Park, M. Yoon, S. Berber, J. Ihm, E. Osawa, and D. Tománek, Phys. Rev. Lett. **91**, 237204 (2003).
[27] K. H. Han, D. Spemann, P. Esquinazi, R. Höhne, V. Riede, and T. Butz, Adv. Mater. (Weinheim, Ger.) **15**, 1719 (2003).
[28] P. Esquinazi, D. Spemann, R. Höhne, A. Setzer, K.-H. Han, and T. Butz, Phys. Rev. Lett. **91**, 227201 (2003).
[29] P. O. Lehtinen, A. S. Foster, Y. Ma, A. V. Krasheninnikov, and R. M. Nieminen, Phys. Rev. Lett. **93**, 187202 (2004).
[30] E. J. Duplock, M. Scheffler, and P. J. D. Lindan, Phys. Rev. Lett. **92**, 225502 (2004).
[31] J. A. Chan, B. Montanari, J. D. Gale, S. M. Bennington, J. W. Taylor, and N. M. Harrison, Phys. Rev. B **70**, 041403(R) (2004).
[32] Y. Ma, P. O. Lehtinen, A. S. Foster, and R. M. Nieminen, Phys. Rev. B **72**, 085451 (2005).
[33] M. Glerup, J. Steinmetz, D. Samaille, O. Stéphan, S. Enouz, A. Loiseau, S. Roth, and P. Bernier, Chem. Phys. Lett. **387**, 193 (2004).
[34] I. Shimoyama, G. Wu, T. Sekiguchi, and Y. Baba, Phys. Rev. B **62**, R6053 (2000).
[35] M. Mehring, W. Scherer, and A. Weidinger, Phys. Rev. Lett. **93**, 206603 (2004).
[36] J. Kotakoski, A. V. Krasheninnikov, Y. Ma, A. S. Foster, K. Nordlund, and R. M. Nieminen, Phys. Rev. B **71**, 205408 (2005).
[37] G. Kresse and J. Furthmüller, Comput. Mater. Sci. **6**, 15 (1996).
[38] G. Kresse and J. Furthmüller, Phys. Rev. B **54**, 11169 (1996).
[39] J. P. Perdew, J. A. Chevary, S. H. Vosko, K. A. Jackson, M. R. Pederson, D. J. Singh, and C. Fiolhais, Phys. Rev. B **46**, 6671 (1992).
[40] G. Kresse and D. Joubert, Phys. Rev. B **59**, 1758 (1999).
[41] P. E. Blöchl, Phys. Rev. B **50**, 17953 (1994).
[42] H. J. Monkhorst and J. D. Pack, Phys. Rev. B **13**, 5188 (1976).
[43] M. W. Zhao, Y. Y. Xia, Y. C. Ma, M. J. Ying, X. D. Liu, and L. M. Mei, Phys. Rev. B **66**, 155403 (2002).
[44] E. Hult, P. Hyldgaard, J. Rossmeisl, and B. I. Lundqvist, Phys. Rev. B **64**, 195414 (2001).
[45] O. A. von Lilienfeld, I. Tavernelli, U. Rothlisberger, and D. Sebastiani, Phys. Rev. Lett. **93**, 153004 (2004).
[46] P. O. Lehtinen, A. S. Foster, A. Ayuela, A. Krasheninnikov, K. Nordlund, and R. M. Nieminen, Phys. Rev. Lett. **91**, 017202 (2003).
[47] D. C. Sorescu, K. D. Jordan, and P. Avouris, J. Phys. Chem. B **105**, 11227 (2001).
[48] P. O. Lehtinen, A. S. Foster, A. Ayuela, T. T. Vehviläinen, and R. M. Nieminen, Phys. Rev. B **69**, 155422 (2004).
[49] G. Mills, H. Jonsson, and G. K. Schenter, Surf. Sci. **324**, 305 (1995).
[50] P. A. Thrower and R. M. Mayer, Phys. Status Solidi A **47**, 11 (1978).
[51] A. V. Krasheninnikov, K. Nordlund, P. O. Lehtinen, A. S. Foster, A. Ayuela, and R. M. Nieminen, Phys. Rev. B **69**, 073402 (2004).
[52] A. S. Ferlauto, A. Champi, C. A. Figueroa, C. T. M. Ribeiro, F. C. Marques, and F. Alvarez, J. Non-Cryst. Solids **338–340**, 486 (2004).
[53] S. Talapatra, P. G. Ganesan, T. Kim, R. Vajtai, M. Huang, M. Shima, G. Ramanath, D. Srivastava, S. C. Deevi, and P. M. Ajayan, Phys. Rev. Lett. **95**, 097201 (2005).
[54] Y. Yagi, T. M. Briere, M. H. F. Sluiter, V. Kumar, A. A. Farajian, and Y. Kawazoe, Phys. Rev. B **69**, 075414 (2004).
[55] P. Krüger, A. Rakotomahevitra, J. C. Parlebas, and C. Demangeat, Phys. Rev. B **57**, 5276 (1998).
[56] E. Durgun, S. Dag, V. M. K. Bagci, O. Gülseren, T. Yildirim, and S. Ciraci, Phys. Rev. B **67**, 201401(R) (2003).
[57] L. Chen, R. Wu, N. Kioussis, and J. R. Blanco, J. Appl. Phys. **81**, 4161 (1997).